Identification of FTIR Bands Due to Internal Water Molecules around the Quinone Binding Sites in the Reaction Center from Rhodobacter sphaeroides

ARTICLE *in* BIOCHEMISTRY · FEBRUARY 2009

Impact Factor: 3.02 · DOI: 10.1021/bi801990s · Source: PubMed

4 AUTHORS, INCLUDING:

Tatsuya Iwata
Nagoya Institute of Technology
34 PUBLICATIONS **774** CITATIONS
SEE PROFILE

Mark L Paddock
University of California, San Diego
107 PUBLICATIONS **3,338** CITATIONS
SEE PROFILE

Melvin Y Okamura
University of California, San Diego
132 PUBLICATIONS **7,709** CITATIONS
SEE PROFILE

Published in final edited form as:
Biochemistry. 2009 February 17; 48(6): 1220–1229. doi:10.1021/bi801990s.

Water Molecules around Quinone Binding Sites in the Reaction Center from *Rhodobacter sphaeroides*

Tatsuya Iwata[‡], **Mark L. Paddock**[§], **Melvin Y. Okamura**[§], and **Hideki Kandori**[*,‡]
Department of Materials Science and Engineering, Nagoya Institute of Technology, Showa-ku, Nagoya 466-8555, Japan, and Department of Physics, University of California at San Diego, 9500 Gilman Drive, La Jolla, CA 92093

Abstract

The photosynthetic bacterial reaction center (RC) is a membrane protein complex. The RC performs the photochemical electron transfer from the bacteriochlorophyll dimer through a series of electron donor and acceptor molecules to a secondary quinone, Q_B. Q_B accepts electrons from a primary quinone, Q_A, in two sequential electron transfer reactions. The second electron transfer to Q_B is coupled to the uptake of two protons from the cytoplasmic side, leading to the formation of the dihydroquinone Q_BH_2 that diffuses out of the RC. The proton uptake pathway in the RC remains unclear, but it has been suggested that water molecules are protonated upon the quinone reduction by the IR continuum bands around 2800-2600 cm^{-1} [Breton, J., and Nabedryk, E. (1998) *Photosyn. Res. 55*, 301–307]. In order to detect structural changes of water molecules upon the reduction of quinones, the wild-type (WT) RC and the site-directed mutants from *Rhodobacter sphaeroides* were measured by means of FTIR spectroscopy in the O-H and O-D stretching regions. In order to investigate the involvement of water molecules to proton uptake, Q_B-/Q_B spectra of WT RC, EQ-L212, DN-L213 and SA-L223 mutants were compared, whose amino acid residues are crucial for the uptake of protons into Q_B. Water stretching vibrations were assigned by use of $H_2{}^{18}O$. The spectra of DN-L213 and SA-L223 look similar to that of WT, whereas the water bands were influenced for EQ-L212. This result suggests that the water molecule(s) is located near Glu-L212. Such structural changes of water molecules are involved in the rearrangement of hydrogen-bonding network around Q_B and Glu-L212, which may play an important role in proton transfer to Q_B-. On the other hand, the continuum bands in the 2800-2600 cm^{-1} region do not originate from water molecules in the Q_A- and Q_B- states. There are no protonated water molecules in the Q_A- and Q_B- states. The bands at 2800-2600 cm^{-1} may originate from N-H stretches which form strong hydrogen bonds. Possible candidate and the hydrogen-bonding environment will be discussed.

The photosynthetic bacterial reaction center (RC)[1] is a membrane protein complex with redox components. The RC of purple bacteria works as a proton pump from cytoplasmic side to the periplasmic side in cooperation with cytochrome bc_1 complex. The RC performs the photochemical electron transfer from the bacteriochlorophyll dimer, P870, through a series of electron donor and acceptor molecules to the secondary quinone, Q_B. Q_B accepts electrons from the primary quinone Q_A in two sequential electron transfer reactions. The second electron transfer to Q_B is coupled to the uptake of two protons from the cytoplasmic side, leading to the formation of the dihydroquinone Q_BH_2 that diffuses out of the RC (reviewed in refs 1,2). The formation of the proton gradient across membranes is essential process for ATP synthesis.

*To whom correspondence should be addressed. Phone & FAX: 81-52-735-5207. E-mail: E-mail: kandori@nitech.ac.jp.
‡Nagoya Institute of Technology
§University of California at San Diego

[1]Abbreviations: RC, reaction center; Q_A, primary quinone; Q_B, secondary quinone; *Rb.*, *Rhodobacter*; FTIR, Fourier transform infrared;

In the photosynthetic RC of purple bacteria, Q_B is buried in the protein and it is suggested that amino acid side chains and internal water molecules are involved in the proton uptake process from the cytoplasmic side.

The pathway of protons must exist from the cytoplasm to the Q_B binding site because Q_B is buried inside the protein and not exposed in the cytoplasmic side. Site-directed mutant studies revealed that three amino acid residues, Glu-L212 (3–5), Asp-L213 (4,6,7) and Ser-L223 (8, 9) play an essential role in donation of protons to reduced Q_B of *Rhodobacter* (*Rb.*) *sphaeroides*. The crystal structure of the RC shows that there are hydrophilic pathways which contain protonatable amino acid residues and water molecules from the cytoplasm to the Q_B binding site (10,11). It is thought that protons are transported through protonation/deprotonation of these amino acid side chains to Q_B. Actually, when mutations are introduced into amino acids (Asp-M17, Asp-L210, His-H126 and His-H128), the rates of proton uptake and accompanying electron transfer from Q_A- to Q_B (and Q_B-) are reduced (12,13) (Figure 1).

Protonation states of carboxylic acid side chains have been studied by light induced Fourier transform infrared (FTIR) spectroscopy because the infrared signals are sensitive to the protonation states of glutamic acid and aspartic acid, whose C=O stretch of protonated carboxylic acid side chain appear in the 1770-1700 cm^{-1} region. However, the pathway of protons from cytoplasmic side to the inside of the RC remains unclear because the signal of protonation is not observed except for Glu-L212 upon the reduction of Q_B (14–18). Moreover, the protonation signal of the acid amino acid residue side chain is not observed in the RC of *Blastochloris viridis* (19). Is proton uptake into the protein carried out without passing through the amino acid side chains?

One possibility is that water molecules which form hydrogen-bonding network from cytoplasm to Q_B site mediates proton transfer upon the quinone reduction (Figure 1). Breton and Nabedryk insist water protonation because the IR signals appear in 2800-1900 cm^{-1} region and are H/D exchangeable (20). Hermes et al. observed similar signals in DN-L210 mutant by time-resolved FTIR studies (21). Indeed, in bacteriorhodopsin, a light-driven proton pump, protonation of internal water molecule (Zundel cation, $H_5O_2^+$) has been proposed as a proton release group detected in the 2000-1900 cm^{-1} region (22,23). However, those bands do not originate from the protonated water just because it appears in such low frequency region. In bacteriorhodopsin, the O-H stretching vibration of the water molecule that bridges positive and negative charges appears at 2800 cm^{-1} (24–26). Isotope water in the oxygen atom must be used in order to prove water signals.

We are interested in hydrogen bonding environment of internal water molecules upon the uptake of protons in the bacterial RC as well as water protonation, for our group has been shown the importance of internal water molecules in the proton transfer processes of bacteriorhodopsin by means of FTIR spectroscopy (24–26, reviewed in refs 27,28 and references therein). FTIR spectroscopy is a powerful tool to detect changes of hydrogen-bond environment as well as the protonation state of carboxylic residues. We researched with the aim of detecting structural changes in internal water molecules accompanied by the reduction of quinones in the RC.

In this study, we confirmed that dry-hydrated films work almost normally as in the solution by FTIR spectroscopy. The changes of water O-H stretches were detected upon the reduction of Q_A and Q_B, respectively in 3700-3500 cm-1 region. Mutational measurement suggested that water molecules existed in the neighborhood of Glu-L212. On the other hand, continuum bands in the 3000-2600 cm^{-1} region did not show spectral shifts by $H_2{}^{18}O$ isotope, suggesting that these bands do not originate from (protonated) water. These suggest the possibility to be the N-H group(s) which forms strong hydrogen bonds.

Materials and Methods

The construction of the site-directed mutant EQ-L212, DN-L213 and SA-L223 was previously reported (3,7,8). The purification of RCs was carried out as is in ref 7. RCs were dialyzed against dialysis buffer (10 mM Tris·HCl (pH8), 0.1 mM EDTA·2Na, 5 mM NaCl, and 0.02 % (w/v) dodecyl maltopyranoside). 15 μL of RC (70–100 μM) and 5 μL of reducing reagents mixture (10 mM sodium ascorbate, 20 mM 2,3,5,6-tetramethyl-*p*-phenylendiamine in 10 mM Tris·HCl (pH8), 1 mM EDTA·2Na, 0.025% (w/v) *N*,*N*-dimethyldodecylamine N-oxide) were mixed. For Q_A measurement, terbutryn was added to a final concentration of 100 μM. For Q_B measurement, 10 μL of ubiquinone-10 (1 mg/mL in ethanol) was added the RC mixture. The RC mixtures were put on a BaF_2 window and dried by aspiration. The RC films were rehydrated by placing ~1 μL of 20% (v/v) glycerol/water (H_2O or $H_2{}^{18}O$) aside.

H/D exchange was carried out by diluting the RC sample with dialysis buffer prepared in D_2O and concentrating by Amicon YM-30 device (Millipore) for three times. The RC in D_2O buffer was incubated for 16 hours at 293 K according to the ref 13. For Q_A and Q_B measurements, the same reagents were added as D_2O-treated samples and dried on a BaF_2 window. The RC films were rehydrated by 20% (v/v) glycerol-$(OD)_3$/water (D_2O or $D_2{}^{18}O$).

Light-induced Q_A-/Q_A difference spectra were measured at 283 K under continuous illumination of >700 nm light (R69 and C40B, Asahi Thechno Glass) with a 1 kW tungsten lump (29). Light intensity was decreased to 0.5% by the use of ND filters for Q_B-/Q_B measurements (30). For FTIR spectra, 256 interferograms at 2 cm^{-1} resolution were recorded during and before illumination, after and during illumination. By subtracting difference spectra after and during illumination from difference spectra during and before illumination, baseline drift was efficiently eliminated. 80–100 recordings were averaged.

Results

The Q^-/Q difference FTIR spectra of the rehydrated RC films

Figure 2a and b show the Q_A-/Q_A and Q_B-/Q_B difference spectra of the WT RC films in the 1800-1200 cm^{-1} region, respectively. In Figure 2a, a characteristic positive band at 1467 cm^{-1} is observed in the Q_A-/Q_A spectrum, which comes from C_1=O stretch (31) or C_4=O stretch (32) of semiquinone. The bands at 1735 (-)/1729 (+) cm^{-1} are reported to the 10a-ester C=O stretch of bacteriopheophytin (33). The negative band at 1670 cm^{-1} is assigned to amide-I C=O stretch (31). These are characteristic to Q_A-/Q_A spectrum previously reported (28, 30–32). Similarly, a positive peak at 1478 cm^{-1} for the Q_B-/Q_B spectrum comes from C=O/C=C stretch of semiquinone (34, 35). The negative peak at 1641 cm^{-1} originates from C=O groups of neutral Q_B (34, 35). The positive band at 1728 cm^{-1} comes from C=O group of protonated carboxylic acid side chain of Glu-L212 (14). Thus, the dry-hydrated films work almost normally as in the solution. We are able to investigate higher frequency region.

The Q^-/Q difference FTIR spectra in the 3700-3490 cm^{-1} region

Figure 3a shows Q_A-/Q_A spectrum of the WT RC in the 3700-3490 cm^{-1} region. Q_A-/Q_A spectrum hydrated with H_2O (red line) has peaks at 3664 (+), 3657 (−), 3622 (−), 3587 (−) and 3501 (+) cm^{-1}. Of those, the bands at 3664 (+), 3657 (−), 3622 (−) and 3587 (−) cm^{-1} spectral shifts by 10–11 cm^{-1} by the hydration of $H_2{}^{18}O$ (blue line), indicating that these bands originate from water stretching vibrations upon the formation of Q_A-. The band at 3664 (+) cm^{-1} remains in the $H_2{}^{18}O$-hydrated sample. This is probably because multiple signals appear in the same frequency region and an exchangeable water molecule shows downshift, or because the efficiency of substitution to $H_2{}^{18}O$ was low. If the band at 3664 (+) cm^{-1} is attributed to remaining $H_2{}^{16}O$, the contribution should be subtracted by use of $H_2$16O spectrum. The black

line in Figure 3b shows the calculated spectrum so that the band at 3664 (+) cm^{-1} was disappeared. Contribution of ^{16}O-H stretch was estimated to be 50%, that is, the efficiency of $H_2{}^{18}O$ replacement was 50% in this experiment.

Similarly, Q_B-/Q_B spectrum hydrated with H_2O has peaks at 3632 (+), 3618 (−) and 3543 (+) cm^{-1} and show $H_2{}^{18}O$ isotope shift at 3618 (−) and 3543 (+) cm^{-1} (Figure 3c). The shifted bands originate from water stretch vibrations. On the other hand, the band at 3632 (+) cm^{-1} looks unshifted, but reduced by $H_2{}^{18}O$ hydration. We supposed that the enough shift was not observed because the substitution efficiency of $H_2{}^{18}O$ was low as well as the Q_A-/Q_A spectrum, and the contribution of $H_2{}^{16}O$ was deducted (black line in Figure 3d). In the case of Q_B-/Q_B spectrum, the substitution efficiency of $H_2{}^{18}O$ was estimated as 45%.

The signals appearing in this region represent weakly hydrogen-bonded X-H groups. It shows that the water molecules are located in the hydrophobic environment, or that they are in hydrophilic environment but the O-H stretch does not form hydrogen bond. Those water molecules are expected to be inside protein. The substitution efficiency of the water ^{18}O whose O-H stretch appears in such an environment is approximately 50% by the operation of hydration.

IR spectra could be detected water molecules around quinones whose environment of is different from each other. We can distinguish both Q-/Q spectra in this frequency region clearly as well as in the 1800-1200 cm^{-1} region. The band at 3501 (−) cm^{-1} in the Q_A-/Q_A spectra, which did not show isotope shift by $H_2{}^{18}O$, probably comes from O-H or N-H stretch of apoprotein.

Mutational Effect for Q_B-/Q_B spectra in the 3700-3490 cm^{-1} region

Next, we measured Q_B-/Q_B spectra of SA-L223, DN-L213 and EQ-L212 mutants. In the 1800-1200 cm^{-1} region, difference spectrum of SA-L223 has smaller changes in the amide I region compared with that of WT (Figure 2c) (36). Difference spectrum of DN-L213 has a new peak at 1490 cm^{-1}, where the WT spectrum has only a shoulder of the band at 1479 cm^{-1} (Figure 2d) (14, 16). In the difference spectrum of EQ-L212, the band at 1728 (+) cm^{-1} disappeared and smaller bands at 1739 (−)/1731 (+) cm^{-1} remain (Figure 2e). The band at 1728 (+) cm^{-1} is assigned as C=O stretch of protonated Glu-L212 side chain (14). These spectra reproduce as previously reported spectra measured in solution. Thus, those spectra obtained by dry-hydrated films were similar as those previously reported in the 1800-1200 cm^{-1} region.

Figure 4a–c shows Q_B-/Q_B spectra of SA-L223, DN-L213 and EQ-L212 in the 3700-3490 cm^{-1} region, respectively. All spectra have one negative and two positive peaks (Figure 4a–c, red lines). They were assigned as water O-H stretches because the bands showed downshift by the hydration of $H_2{}^{18}O$ (Figure 4a–c, blue lines). The overall spectral shapes look similar between WT and mutants, the peak frequencies of EQ-L212 are different from those of WT. Figure 4d-f compares mutant spectra with WT spectrum. Water bands appear at 3632 (+), 3618 (−) and 3543 (+) cm^{-1} for SA-L223, which are identical with WT (Figure 4d). These water bands are not influenced by the mutation at Ser-L223, suggesting that these water molecules are not located near Ser-L223. The spectrum of DN-L213 has peaks at 3632 (+), the bands at 3619 (−) and 3543 (+) cm^{-1} (Figure 4e). Though a negative band showed 1 cm^{-1} shift compared with that of WT, it suggests that those water molecules are not influenced by the mutation at Asp-L213. On the other hand, the in the positive bands of EQ-L212 spectrum has obvious shifts to the higher frequency by 5 cm^{-1} compared with WT spectrum (Figure 4f). The negative peak showed 2 cm^{-1} shift to higher frequency. Because these bands were influenced of the mutation at Glu-L212, the water molecules which showed structural changes suggest that the water molecules are located near Glu-L212.

Hermes et al. reported the existence of a band of water at 3681 cm^{-1} for the DN-L210 mutant (21), but we could not find any bands in the 4000-3700 cm^{-1} region for the RCs used in this study (data not shown). This may be specific to the DN-L210 mutant.

Continuum bands in the 2900-2200 cm^{-1} region

Figure 5a and b shows Q_A-/Q_A and Q_B-/Q_B difference FTIR spectra of WT RC in the 2900-2200 cm^{-1} region. In the Q_A-/Q_A spectrum of WT, there are positive peaks at 2818, 2756, 2709, 2611 and 2559 cm^{-1} (Figure 5a). Similarly, Q_B-/Q_B spectrum of WT has a main peak at 2613 cm^{-1} and small peaks at 2831, 2764, 2691 and 2559 cm^{-1} (Figure 5b). The broad bands were reproduced previously reported spectra (20, 37), which originate from O-H stretches of protonated water molecules. Recently, the same group proposed that some part of the band in the Q_A-/Q_A spectrum originates from strongly hydrogen-bonded N_π-H group of His-M219 (38). Anyway, if the bands originate from protonated water molecules, spectral shifts should be observed by the hydration of $H_2{}^{18}O$. The expected downshifts at 2611 (2613) cm^{-1} by $H_2{}^{18}O$ is ~8.5 cm^{-1}, calculated from the square root of reduced mass ratio between ^{16}O-H and ^{18}O-H. The broad bands in the 2600 cm^{-1} region did not show any shift by hydration of $H_2{}^{18}O$ water (blue lines in Figure 5a, b).

Are spectral shifts really observed for such broad bands by comparison of H_2O-hydrated and $H_2{}^{18}O$ hydrated spectra in this experiment? If the half of the signal does not come from O-H stretches of water molecules as is proposed (38), the apparent shift width by $H_2{}^{18}O$ hydration may become smaller. Furthermore, the band shift may not be detected for the H_2O/$H_2{}^{18}O$ exchange when the substitution efficiency of H_2O/$H_2{}^{18}O$ in the higher frequency region is 50% is taken into account (Figure 3). However, the substitution efficiency of the water molecules observed at higher frequencies is 50% and expects that it are substituted for the high efficiency more as for the water molecules in the more hydrophilic environment (Figure 1).

In order to investigate whether the spectral shifts are observed for the Q_B-/Q_B spectra, the following calculation was carried out (Figure 5c–e). We supposed that a half of the band originates from water stretch vibrations and the rest does not. The water signal was simulated by gauss function. We assumed that the gauss function covers the whole region of the band whose peak position and half maximum full width are 2596.7 cm^{-1} and 320 cm^{-1}, respectively (Figure 5c, red solid line). The difference spectrum corresponds to the signal which does not originate from water (Figure 5c, black line). The $H_2{}^{18}O$ spectrum downshifts by 8.5 cm^{-1}, that is, it has a peak at 2588.2 cm^{-1} (Figure 5c, blue line). Because the substitution efficiency of $H_2{}^{18}O$ is 50%, the simulated $H_2{}^{18}O$-hydrated spectrum is the sum of black spectrum, 50% of blue spectrum and 50% of red spectrum (Figure 5d, blue line). When the simulated spectra (Figure 5d) are compared with the measured spectra (Figure 5b), the difference of the both spectra is hardly observed. Figure 5e shows the double difference spectra of the H_2O and the $H_2{}^{18}O$ spectra. Black and red lines in Figure 5e show the double-difference spectra of measured spectra Figure 5b and simulated spectra in Figure 5d, respectively. The result of the simulation cannot be distinguished from the difference in noise level of the measurement. Is it unacceptable to prove that experimentally?

Therefore, hydration by D_2O/$D_2{}^{18}O$ was carried out. The difference in O-D stretching vibration of D_2O and $D_2{}^{18}O$ is expected ~15 cm^{-1}, which is larger than O-H stretches. Figure 6a and b shows the Q_A-/Q_A and Q_B-/Q_B spectra hydrated with D_2O (red lines) and $D_2{}^{18}O$ (blue lines). The broad bands were observed which has peak of 2138 cm^{-1} in the Q_A-/Q_A (Figure 6a) and 2085 cm^{-1} in the Q_B-/Q_B (Figure 6b) spectra. However, it does not seem that these bands shift by the $D_2{}^{18}O$ hydration. It was simulated whether the shifts are observed in the case of D_2O hydration as well as in the case of H_2O hydration for the Q_B-/Q_B spectra.

The same simulation was carried out for D_2O-hydrated spectra as well as H_2O-hydrated ones for the Q_B-/Q_B spectra. The band at 2085 cm^{-1} is expected to the downshift by 15 cm^{-1} by the hydration of $D_2{}^{18}O$. We assumed that a part of the band originates from water and the rest does not. Water band was simulated as a gauss function whose peak and half width full maximum are 2060 cm^{-1} and 133 cm^{-1}, respectively (Figure 6c, red line). The difference spectrum corresponds to the signal which does not originate from water (Figure 6c, black line). The $D_2{}^{18}O$ spectrum downshifts by 15 cm^{-1}, that is, it has a peak at 2045 cm^{-1} (Figure 6c, blue line). The simulated $D_2{}^{18}O$-hydrated spectrum is the sum of black spectrum, 50% of blue spectrum and 50% of red spectrum. Figure 6d shows the calculated spectra. The difference of the spectra is observed better than $H_2{}^{18}O$ (Figure 5d). Though the definite shift of a position of the peak was not observed, two spectra do not correspond as much as the simulation of H_2O. Black and red lines in Figure 6e show the differences of measured and simulated spectra, respectively. In this case, the difference of simulated spectra of D_2O and $D_2{}^{18}O$ is observed clearly, while signal is not observed as for the difference in the measured spectra of D_2O and $D_2{}^{18}O$.

The situation was the same as for the Q_A-/Q_A spectrum (data not shown). Therefore, we concluded that this band does not originate from water O-D stretches. In both Q_A- and Q_B-stated, it is unlikely that the continuum bands in the 2800-2400 cm^{-1} region originate from protonated water molecules.

Mutational Influence of the Continuum Bands at Ser-L223, Asp-L213 and Glu-L212

In the Q_B-/Q_B spectra of SA-L223, DN-L213 and EQ-L212 mutants, the continuum bands were observed (Figure 7). The bands showed almost identical peaks as that of WT and no shift by $H_2{}^{18}O$ hydration. This indicated that the band does not originate from water stretch vibrations. The spectrum of SA-L223 corresponds to that of WT well (Figure 7a). This means that there was no influence of the mutation at Ser-L223 position. On the other hand, spectra of DN-L213 and EQ-L212 had difference in comparison with WT (Figure 7b, c). The drift of the baseline was seen though peak positions were unchanged. The disappearance of negative charges at the position of Asp-L213 (in the neutral and reduced Q_B states) or Glu-L212 (in the neutral Q_B state) may influence the bands. However, we concluded that the influence of these mutations was not taken about because the shift of the bands was not observed. The element which is the cause of this signal is not in the neighborhood of Ser-L223 but may be near Asp-L213 and/or Glu-L212.

Discussion

Assignment of water molecules that formed weak hydrogen bonds

In this report, the structural changes of water molecules were detected around Q_A and Q_B upon the reduction of quinones in the reaction centers from *Rb. sphaeroides*. IR spectra could be detected water molecules around quinones whose environment of is different from each other. The change of hydrogen bonds of water molecules was observed around Glu-L212, which is involved in the proton donation into Q_B. Because the mutation of Asp-L213, which is next to Glu-L212, did not influence the structural changes of water molecules, the changed water molecules must be located in the neighborhood of Glu-L212. It may be reasonable that SA-L223 mutant does not affect the water structural changes upon the formation of Q_B-because Ser-L223 is not involved in the first proton uptake pathway (2 and references therein).

The X-ray crystarography analysis shows that Q_B is located in the distal and proximal sides from His-L190 in the neutral and reduced states, respectively (10). This does not correspond to the result shown by FTIR study, and this is the problem under debate that the Q_B location

in the distal side is specific in the crystal (39). Figure 8 shows the structure of RC of *Rb. sphaeroides* in the Q_A and Q_B binding regions in the charge neutral state (10).

Comparing Figure 8 with Figure 1, there are water molecules in the neighborhood of Glu-L212 under in both neutral Q_B and Q_B- states (water2, 5, 118 and 391). However, we cannot conclude that they are the identical water molecules because the rearrangement of water molecules takes place upon the Q_B movement from "distal side" to "proximal side" from His-L190. And regardless of the correctness of this model, the rearrangement of the water molecules can happen because measurements are carried out at 283 K. The side chain of Glu-L212 is protonated under the Q_B- state. Water molecules are influenced of the disappearance of negative charge at Glu-L212, and change the hydrogen-bonding environment. These water molecules may be involved in the stabilization of Q_B- state and of the protonation of Glu-L212 by changing the hydrogen-bonding environment.

On the other hand, there is smaller number of water molecules in the neighborhood of Q_A. Water molecules exist in the region surrounded by Ala-M249, Asn-M259, Thr-M261 and Phe-L5 (water 82, 409 and 410) (Figure 8). These water molecules are primary candidates which appear in 3700-3500 cm^{-1} region because they are under the hydrophobic environment and possibly influenced by the Q_A-formation.

The structural changes of water molecules that form weak hydrogen bond upon the reduction of quinones

The broad bands in the 2800-2400 cm^{-1} region do not originate from water molecules in the Q_A- and Q_B- states. There are no protonated water molecules in the Q_A- and Q_B- states.

The bands at 2800-2400 cm^{-1} may originate from N-H stretches which form strong hydrogen bonds. It was previously assigned that the N-H stretch of protonated Schiff base in bacteriorhodopsin in the ground state appear at 2800 cm^{-1} with broad bandwidth (40). This is characteristic to the strongly hydrogen-bonded N-H groups. And in the Q_A-/Q_A FTIR difference spectra of photosystem II, multiple peaks in the 3000-2600 cm^{-1} originate from strongly hydrogen-bonded histidines (41). Taking those observations and the result of Breton et al. (38) into account, all band observed in the Q_A-/Q_A spectrum could originate from the strongly hydrogen-bonded N_p-H group of His-M219 (Figure 8). Similar peaks are also observed in the Q_B-/Q_B spectrum to that of Q_A-/Q_A. We assume that the bands originate from N-H group which is positively charged or which forms strongly hydrogen bonds with negatively charged groups. Possible candidate is His-L190 (strongly hydrogen-bonded with negatively charged Q_B-) (Figure 1). Such a strong hydrogen bond could be involved in the proton donation from Glu-L212 as well as the rearrangement of water molecules.

The distance between N_π atom of His-L190 and carboxyl oxygen atom of Glu-L212 and between His-L190 and Asp-L213 are 6.0 (6.3) and 9.8 (10.3) Å in the unphotolyzed (charge separated) state, respectively (Figures 9 and 1). Because the charged Q_A- or Q_B- can influence the structural change in the position at Asp-L210, whose distances are 25 and 10.5 Å, respectively (37), it may be possible that (the loss of) the negative charge at the position of Glu-L212 or Asp-L213 influences N_π-H group of His-L190.

Iron-substituted RCs (42) and site-directed mutants would be useful for the identification of those bands. IR spectra in the higher frequency region would give us much more information about hydrogen-bonding environment of charge separated states in RCs as well as of intermediates in bacteriorhodopsin.

References

1. Okamura MY, Feher G. PROTON TRANSFER IN REACTION CENTERS FROM PHOTOSYNTHETIC BACTERIA. Annu Rev Biochem 1992;61:861–896. [PubMed: 1323240]
2. Okamura MY, Paddock ML, Graige MS, Feher G. Proton and electron transfer in bacterial reaction centers. Biochim Biophys Acta 2000;1458:148–163. [PubMed: 10812030]
3. Paddock ML, Rongey SH, Feher G, Okamura MY. Pathway of proton transfer in bacterial reaction centers: Replacement of glutamic acid 212 in the L subunit by glutamine inhibits quinone (secondary acceptor) turnover. Proc Natl Acad Sci USA 1989;86:6602–6606. [PubMed: 2570421]
4. Takahashi E, Wraight CA. Proton and Electron Transfer in the Acceptor Quinone Complex of *Rhodobacter sphaeroides* Reaction Centers: Characterization of Site-Directed Mutants of the Two Ionizable Residues, Glu^{L212} and Asp^{L213}, in the Q_B Binding Site. Biochemistry 1992;31:855–866. [PubMed: 1731944]
5. Shinkarev VP, Takahashi E, Wraight CA. Flash-induced electric potential generation in wild type and L212EQ mutant chromatophores of *Rhodobacter sphaeroides*: QBH2 is not released from L212EQ mutant reaction centers. Biochim Biophys Acta 1993;1142:214–216.
6. Takahashi E, Wraight CA. A crucial role of Asp^{L213} in the proton transfer pathway to the secondary quinone of reaction centers from *Rhodobacter sphaeroides*. Biochim Biophys Acta 1990;1020:107–111.
7. Paddock ML, Rongey SH, McPherson PH, Juth A, Feher G, Okamura MY. Pathway of Proton Transfer in Bacterial Reaction Centers: Role of Aspartate-L213 in Proton Transfers Associated with Reduction of Quinone to Dihydroquinone. Biochemistry 1994;33:734–745. [PubMed: 8292601]
8. Paddock ML, McPherson PH, Feher G, Okamura MY. Pathway of proton transfer in bacterial reaction centers: Replacement of serine-L223 by alanine inhibits electron and proton transfers associated with reduction of quinone to dihydroquinone. Proc Natl Acad Sci USA 1990;87:6803–6807. [PubMed: 2168561]
9. Paddock ML, Feher G, Okamura MY. Pathway of Proton Transfer in Bacterial Reaction Centers: Further Investigations on the Role of Ser-L223 Studied by Site-Directed Mutagenesis. Biochemistry 1995;34:15742–15750. [PubMed: 7495805]
10. Stowell MHB, McPhillips TM, Rees DC, Soltis SM, Abresch E, Feher G. Light-Induced Structural Changes in Photosynthetic Reaction Center: Implications for Mechanism of Electron-Proton Transfer. Science 1997;276:812–816. [PubMed: 9115209]
11. Axelrod HL, Abresch EC, Paddock ML, Okamura MY, Feher G. Determination of the binding sites of the proton transfer inhibitors Cd^{2+} and Zn^{2+} in bacterial reaction centers. Proc Natl Acad Sci USA 2000;97:1542–1547. [PubMed: 10677497]
12. Paddock ML, Äderloth P, Chang C, Abresch EC, Feher G, Okamura MY. Identification of the Proton Pathway in Bacterial Reaction Centers: Cooperation between Asp-M17 and Asp-L210 Facilitates Proton Transfer to the Secondary Quinone (Q_B). Biochemistry 2001;40:6893–6902. [PubMed: 11389604]
13. Äderloth P, Paddock ML, Tehrani A, Beatty T, Feher G, Okamura MY. Identification of the Proton Pathway in Bacterial Reaction Centers: Decrease of Proton Transfer Rate by Mutation of Surface Histidines at H126 and H128 and Chemical Rescue by Imidazole Identifies the Initial Proton Donors. Biochemistry 2001;40:14538–14546. [PubMed: 11724567]
14. Nabedryk E, Breton J, Hienerwadel R, Fogel C, Paddock ML, Okamura MY. Fourier Transform Infrared Difference Spectroscopy of Secondary Quinone Acceptor Photoreduction in Proton Transfer Mutants of *Rhodobacter sphaeroides*. Biochemistry 1995;34:14722–14732. [PubMed: 7578080]
15. Nabedryk E, Breton J, Okamura MY, Paddock ML. Proton Uptake by Carboxylic Acid Groups upon Photoreduction of the Secondary Quinone (Q_B) in Bacterial Reaction Centers from *Rhodobacter sphaeroides*: FTIR Studies on the Effects of Replacing Glu H173. Biochemistry 1998;37:14457–14462. [PubMed: 9772172]
16. Nabedryk E, Breton J, Okamura MY, Paddock ML. Direct evidence of structural changes in reaction centers of *Rb. sphaeroides* containing suppressor mutations for Asp L213 -> Asn: A FTIR study of Q_B photoreduction. Photosyn Res 1998;55:293–299.

17. Nabedryk E, Breton J, Okamura MY, Paddock ML. Simultaneous Replacement of Asp-L210 and Asp-M17 with Asn Increases Proton Uptake by Glu-L212 upon First Electron Transfer to Q_B in Reaction Centers from *Rhodobacter sphaeroides*. Biochemistry 2001;40:13826–13832. [PubMed: 11705371]

18. Nabedryk E, Breton J, Okamura MY, Paddock ML. Identification of a Novel Protonation Pattern for Carboxylic Acids upon Q_B Photoreduction in *Rhodobacter sphaeroides* Reaction Center Mutants at Asp-L213and Glu-L212 Sites. Biochemistry 2004;43:7236–7243. [PubMed: 15182169]

19. Breton, J.; Nabedryk, E.; Mioskowski, C.; Boullais, C. Protein-quinone interactions in photosynthetic bacterial reaction centers investigated by light-induced FTIR difference spectroscopy. In: Michel-Beyerle, M-E., editor. The Reaction Center of Photosynthetic Bacteria, Structure and Dynamics. Springer-Verlag; New York: 1996. p. 381-394.

20. Breton J, Nabedryk E. Proton uptake upon quinone reduction in bacterial reaction centers: IR signature and possible participation of a highly polarizable hydrogen bond network. 1998

21. Hermes S, Stachink JM, Onidas D, Remy A, Hofmann E, Gerwert K. Proton Uptake in the Reaction Center Mutant L210DN from *Rhodobacter sphaeroides* via Protonated Water Molecules. Biochemistry 2006;45:13741–13749. [PubMed: 17105193]

22. Le Courte J, Tittor J, Oesterhelt D, Gerwert K. Experimental evidence for hydrogen-bonded network proton transfer in bacteriorhodopsin shown by Fourier-transform infrared spectroscopy using azide as catalyst. Proc Natl Acad Sci USA 1995;92:4962–4966. [PubMed: 7761432]

23. Garczarek F, Wang J, El-Sayed MA, Gerwert K. The Assignment of the Different Infrared Continuum Absorbance Changes Observed in the 3000-1800-cm^{-1} Region during the bacteriorhodopsin Photocycle. Biophys J 2004;87:2676–2682. [PubMed: 15298873]

24. Kandori H, Shichida Y. Direct Observation of the Bridged Water Stretching Vibrations Inside a Protein. J Am Chem Soc 2000;122:11745–11746.

25. Shibata M, Tanimoto T, Kandori H. Water Molecules in the Schiff Base Region of bacteriorhodopsin. J Am Chem Soc 2003;125:13312–13313. [PubMed: 14582999]

26. Shibata M, Kandori H. FTIR Studies of Internal Water Molecules in the Schiff base Region of Bacteriorhodopsin. Biochemistry 2005;44:7406–7413. [PubMed: 15895984]

27. Kandori H. Role of internal water molecules in bacteriorhodopsin. Biochem Biophys Acta 2000;1460:177–191. [PubMed: 10984599]

28. Furutani Y, Shibata M, Kandori H. Strongly hydrogen-bonded water molecules in the Schiff base region of rhodopsins. Photochem Photobiol Sci 2005;4:661–666. [PubMed: 16121274]

29. Breton J, Thibodeau DL, Berthomieu C, Mäntele W, Verméglio A, Nabedryk E. Probing the primary quinone environment in photosynthesis bacterial reaction centers by light-induced FTIR difference spectroscopy. FEBS Lett 1991;278:257–260. [PubMed: 1899390]

30. Breton J, Berthomieu C, Thibodeau DL, Nabedryk E. Probing the secondary quinone (Q_B) environment in photosynthesis bacterial reaction centers by light-induced FTIR difference spectroscopy. FEBS Lett 1991;288:109–113. [PubMed: 1879543]

31. Breton J, Boullais C, Burie J-R, Nabedryk E, Mioskowski C. Binding Sites of Quinones in Photosynthetic Bacterial Reaction Centers Investigated by Light-Induced FTIR Difference Spectroscopy: Assignment of the Interactions of Each Carbonyl of Q_A in *Rhodobacter sphaeroides* Using Site-Specific ^{13}C-labeled Ubiquinone. Biochemistry 1994;33:14378–14386. [PubMed: 7981197]

32. Brudeler R, de Groot HJM, van Liemt WBS, Steggrerda WF, Esmeijer R, Gast P, Hoff AJ, Lugtenburg J, Gerwert K. Asymmetric binding of the 1- and 4-C=O groups of Q_A in *Rhodobacter sphaeroides* R26 reaction centers monitored by Fourier transform infra-red spectroscopy using site-specific isotopically labeled ubiquinone-10. EMBO J 1994;13:5523–5530. [PubMed: 7988549]

33. Breton J, Nabedryk E, Allen JP, Williams JC. Electrostatic Influence of QA Reduction on the IR Vibrational Mode of the 10a-Ester C=O of H_A Demonstrated by Mutations at Residues Glu L104 and Trp L100 in Reaction Centers from *Rhodobacter sphaeroides*. Biochemistry 1997;36:4515–4525. [PubMed: 9109660]

34. Breton J, Boullais C, Berger G, Mioskowski C, Nabedryk E. Binding Sites of Quinones in Photosynthetic Bacterial Reaction Centers Investigated by Light-Induced FTIR Difference Spectroscopy: Symmetry of the Carbonyl Interactions and Close Equivalence of the Q_B Vibrations

in *Rhodobacter sphaeroides* and *Rhodopseudomonas viridis* Probed by Isotope Labeling. Biochemistry 1995;34:11606–11616. [PubMed: 7547892]

35. Brudler R, de Groot HJM, van Liemt WBS, Gast P, Hoff AJ, Lugtenburg J, Gerwert K. FTIR spectroscopy shows weak symmetric hydrogen bonding of the Q_B carbonyl groups in *Rhodobacter sphaeroides* R26 reaction centres. FEBS Lett 1995;370:88–92. [PubMed: 7649310]
36. Nabedryk E, Paddock ML, Okamura MY, Breton J. An Isotope-Edited FTIR Investigation of the Role of Ser-L223 in Binding Quinone (Q_B) and Semiquinone (Q_B-) in the Reaction Center from *Rhodobacter sphaeroides*. Biochemistry 2005;44:14519–14527. [PubMed: 16262252]
37. Breton J. Steady-State FTIR Spectra of the Photoreduction of Q_A and Q_B in *Rhodobacter sphaeroides* Reaction Centers Provide Evidence against the Presence of a Proposed Transient Electron Acceptor X between the Two Quinones. Biochemistry 2007;46:4459–4465. [PubMed: 17381130]
38. Breton J, Lavergne J, Wakeham MC, Nabedryk E, Jones MR. The Unusually Strong Hydrogen Bond between the Carbonyl of Q_A and His M219 in the *Rhodobacter sphaeroides* Reaction Center Is Not Essential for Efficient Electron Transfer from Q_A- to Q_B. Biochemistry 2007;46:6468–6476. [PubMed: 17497939]
39. Breton J, Boullais C, Mioskowski C, Sebban P, Baciou L, Nabedryk E. Vibrational Spectroscopy Favors a Unique Q_B Binding Site at the Proximal Position in Wild-Type Reaction Centers and in the Pro-L209 -> Tyr Mutant from *Rhodobacter sphaeroides*. Biochemistry 2002;41:12921–12927. [PubMed: 12390017]
40. Kandori H, Belenky M, Heltzfeld J. Vibrational Frequency and Dipolar Orientation of the Protonated Schiff Base in Bacteriorhodopsin before and after Photoisomerization. Biochemistry 2002;41:6026–6031. [PubMed: 11993997]
41. Noguchi T, Inoue Y, Tang X-S. Hydrogen Bonding Interaction between the Primary Quinone Acceptor Q_A and a Histidine Side Chain in Photosystem II as Revealed by Fourier Transform Infrared Spectroscopy. Biochemistry 1999;38:399–403. [PubMed: 9890922]
42. Debus RJG, Feher RJ, Okamura MY. Iron-Depleted Reaction Centers from *Rhodopseudomonas sphaeroides* R-26.1: Characterization and Reconstitution with Fe^{2+}, Mn^{2+}, Co^{2+}, Ni^{2+}, Cu^{2+}, and Zn^{2+} Biochemistry 1986;25:2276–2287. [PubMed: 3011083]

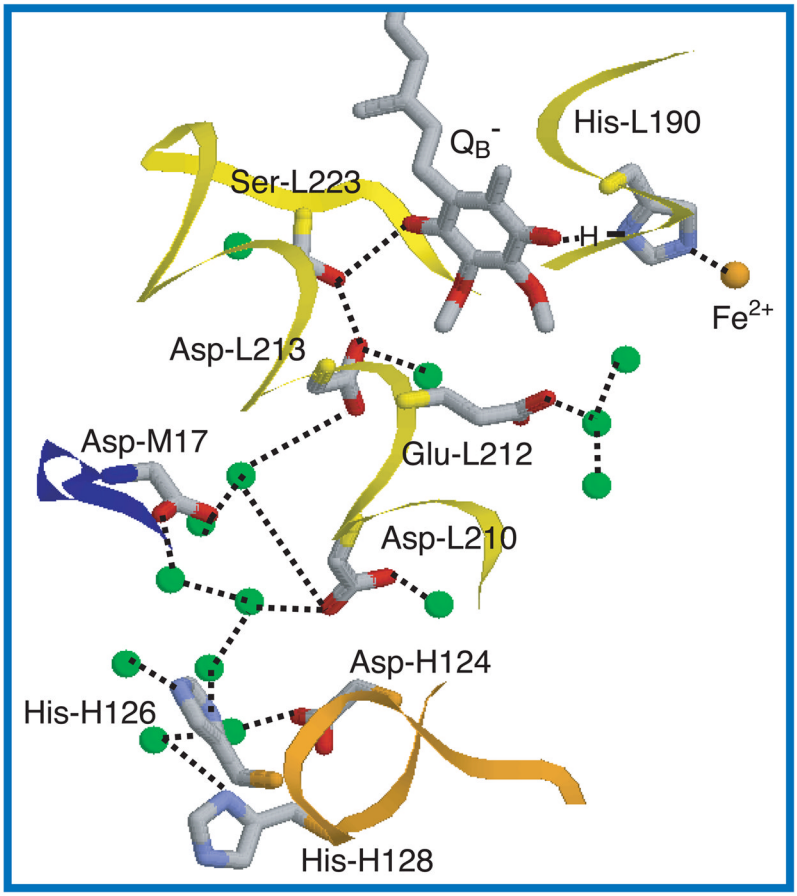

Figure 1.

Structure of Q_B binding site of the reaction center of *Rb. sphaeroides* in the P^+Q_B-state (PDB entry: 1DV3 (11)). Peptide backbones are shown as ribbons, where L, M and H subunits are colored yellow, blue and orange, respectively. Quinone and amino acid side chains are shown as stick drawings. Green shares represent water molecules. Dotted lines show putative hydrogen bonds.

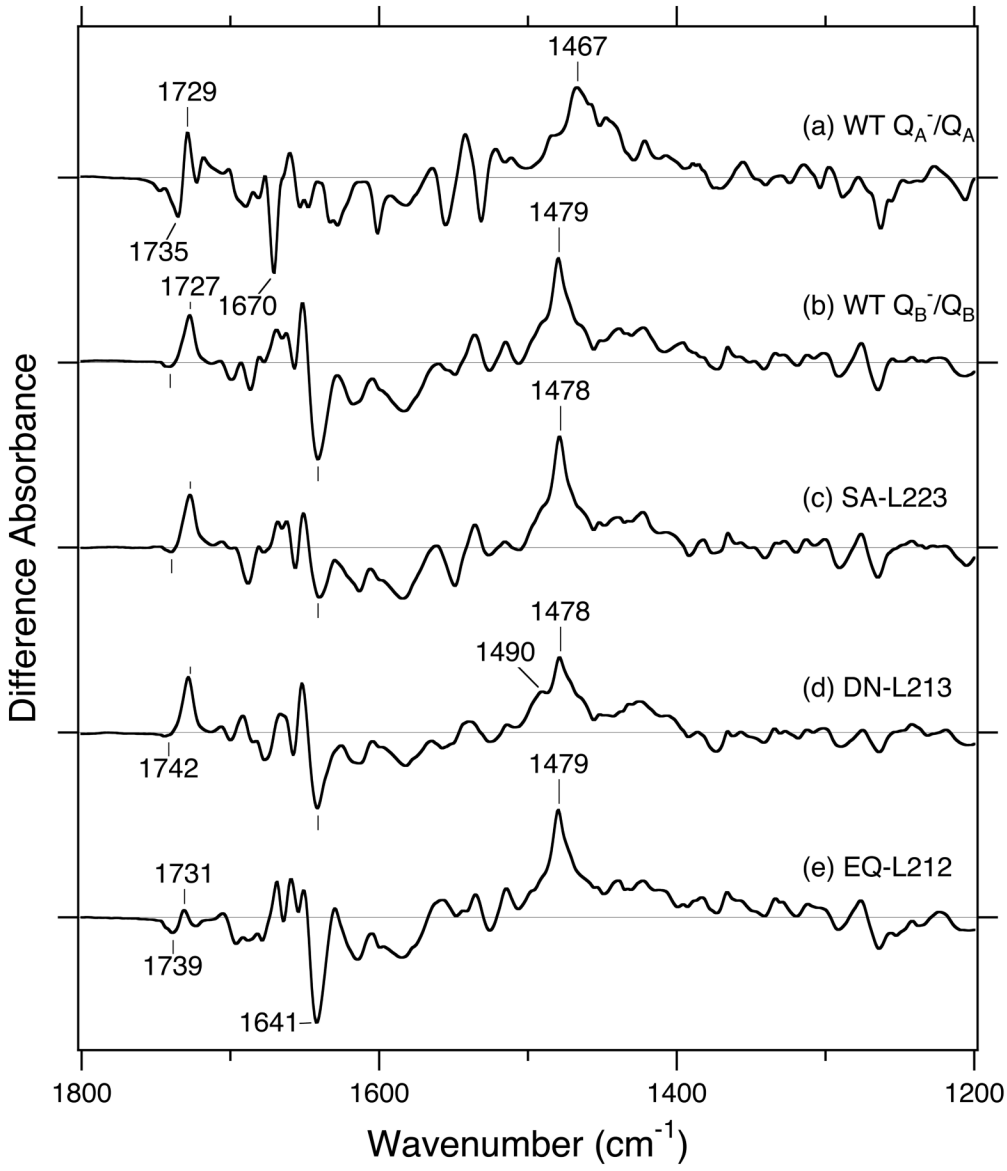

Figure 2.

Light-induced Q^-/Q difference FTIR spectra of *Rb. Sphaeroides* RCs in the 1800-1200 cm^{-1} region. Q_A-/Q_A spectrum of WT (a), Q_B-/Q_B spectra of WT (b), SA-L223 (c), DN-L213 (d) and EQ-L212 (e) are shown. One division of the *y*-axis corresponds to 0.002 absorbance unit.

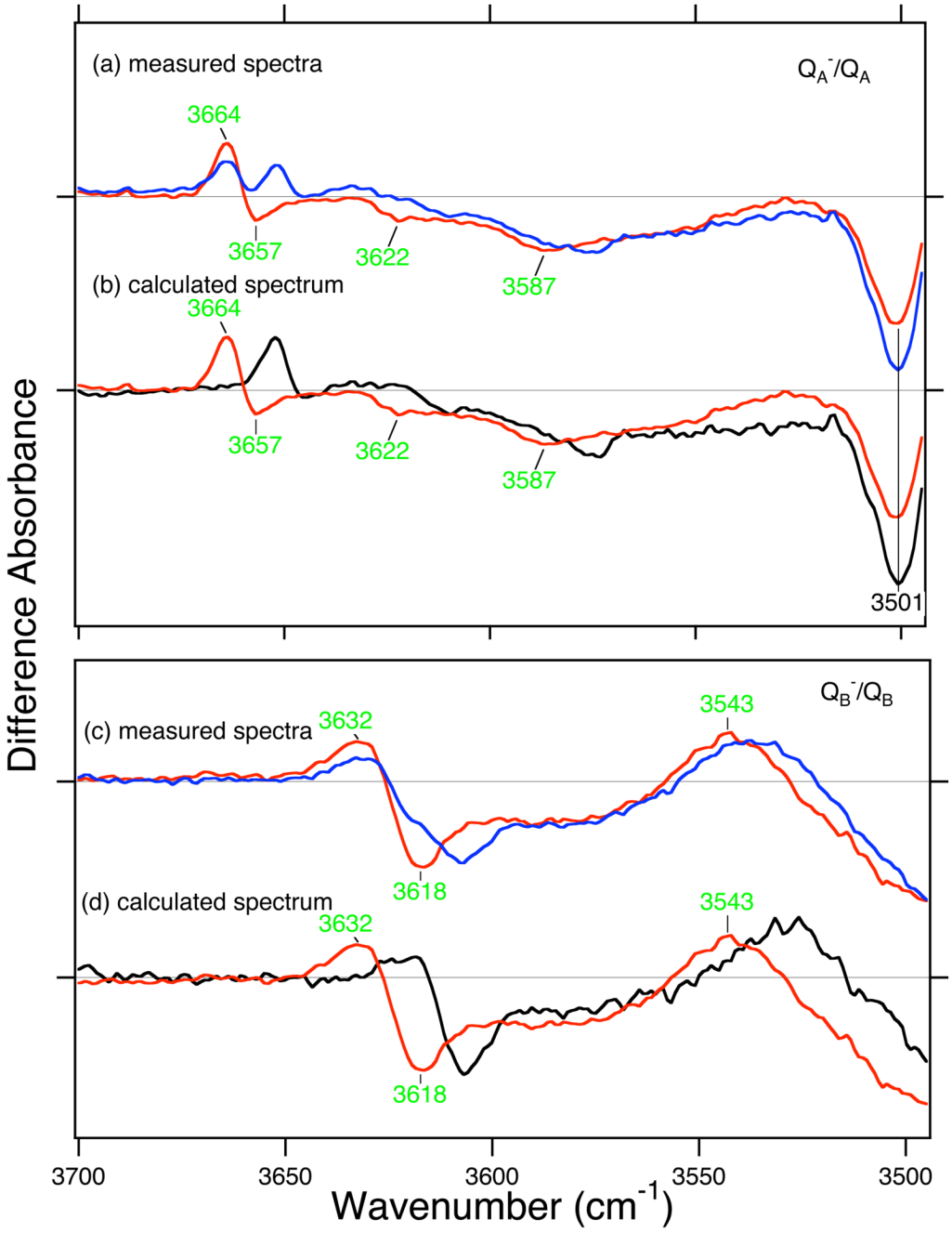

Figure 3.

Light-induced Q_A-/Q_A and Q_B-/Q_B difference FTIR spectra of *Rb. Sphaeroides* WT RCs in the 3700-3490 cm^{-1} region. (a) Q_A-/Q_A difference spectra hydrated with H_2O (red line) or $H_2{}^{18}O$ (blue line). (b) Q_A-/Q_A difference spectra hydrated with H_2O (red line, same as panel a) and calculated Q_A-/Q_A difference spectrum of pure $H_2{}^{18}O$-hydration (black line). (c) Q_B-/Q_B difference spectra hydrated with H_2O (red line) or $H_2{}^{18}O$ (blue line). (d) Q_B-/Q_B difference spectra hydrated with H_2O (red line, same as panel c) and calculated Q_B-/Q_B difference spectrum of pure $H_2{}^{18}O$-hydration (black line). Frequencies labeled in green correspond to those identified as water stretching vibrations. One division of the *y*-axis corresponds to 0.0002 absorbance unit.

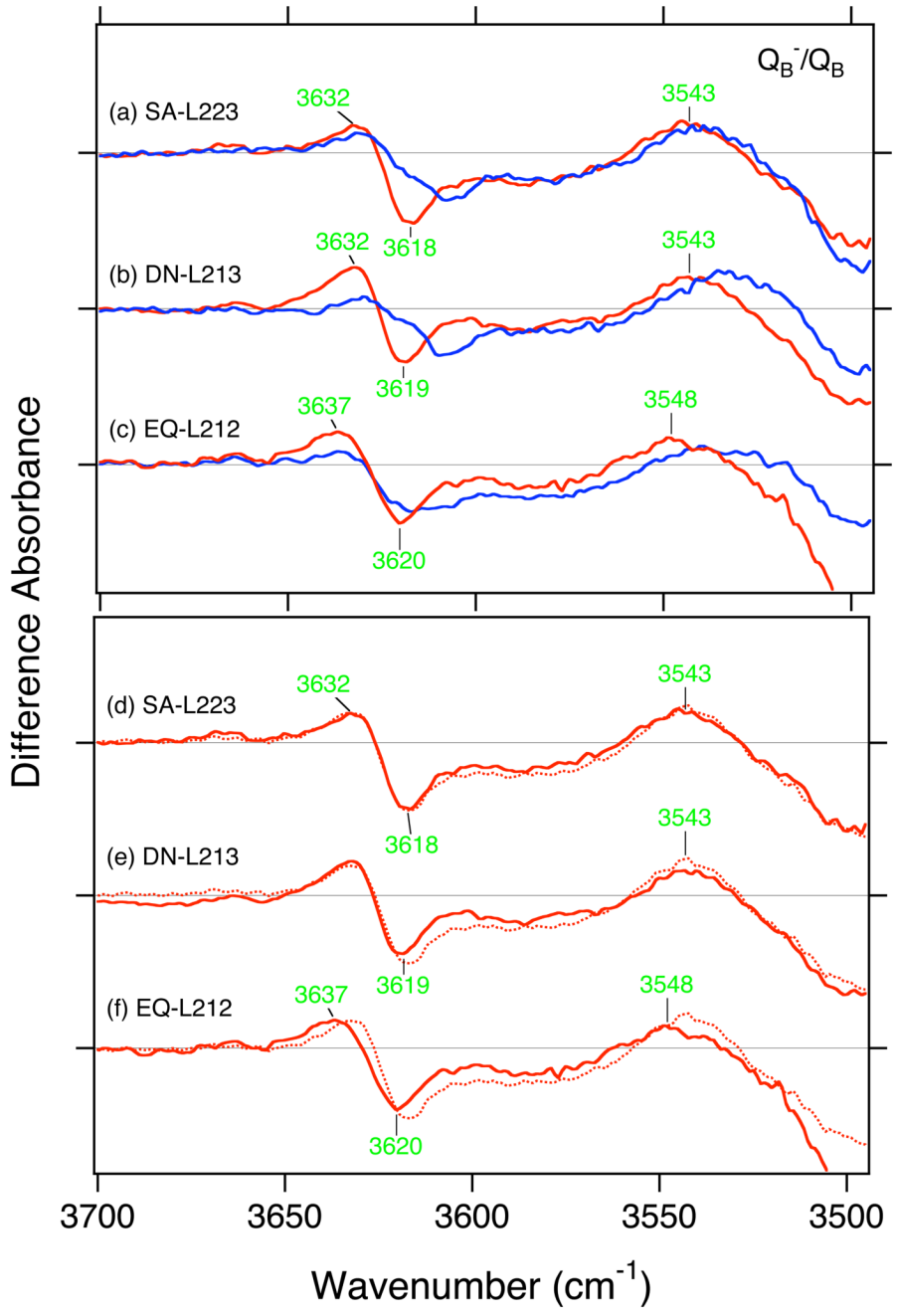

Figure 4.

Light-induced Q_B^-/Q_B difference FTIR spectra of *Rb. Sphaeroides* mutant RCs in the 3700-3490 cm^{-1} region. (a–c) Q_B^-/Q_B spectra of SA-L223 (a), DN-L213 (b) and EQ-L212 (c) hydrated with H_2O (red lines) or $H_2{}^{18}O$ (blue lines). (d–f) Q_B^-/Q_B spectra of SA-L223 (d), DN-L213 (e) and EQ-L212 (f) (solid lines) are compared with the spectrum of WT (dotted lines). The samples are hydrated with H_2O. One division of the *y*-axis corresponds to 0.0002 absorbance unit. Labeled frequencies correspond to those identified as water stretching vibrations.

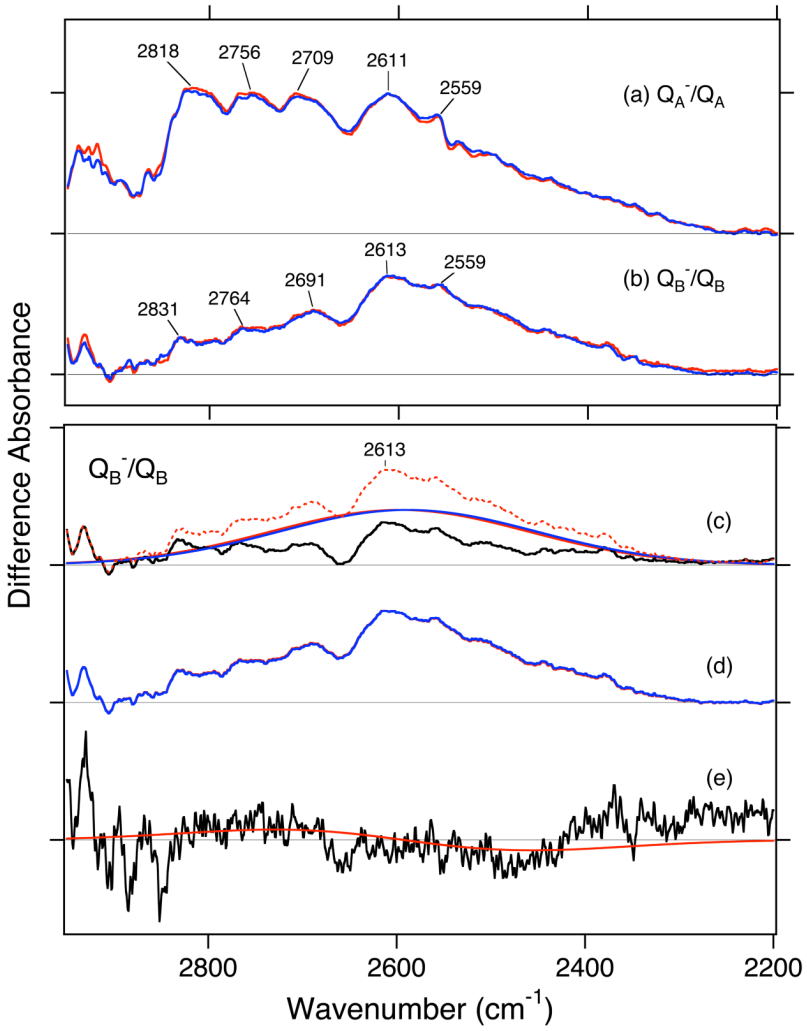

Figure 5.

(a, b) Light-induced Q-/Q difference FTIR spectra of *Rb. Sphaeroides* RCs in the 2950-2200 cm^{-1} region. (a) Q_A-/Q_A and (b) Q_B-/Q_B spectra of WT. Samples are hydrated with H_2O (red line) or $H_2{}^{18}O$ (blue line). (c–e) Simulation of the continuum bands of Q_B-/Q_B spectra. (c) (red dotted line) WT Q_B-/Q_B spectrum. (red solid line) The Gaussian function whose position and half maximum full width are 2596.7 cm^{-1} and 320 cm^{-1}, respectively. (black line) The difference spectrum between red dotted spectrum and red solid spectrum. (blue line) The Gaussian function whose position and half maximum full width are 2588.2 cm^{-1} and 320 cm^{-1}, respectively. Red and blue solid lines mimic H_2O and $H_2{}^{18}O$ bands, respectively, and black line mimics the bans which are not originate from water, such as N-H stretch (38). (d) (red line) WT Q_B-/Q_B spectrum (sum of red solid line and black line in panel c). (blue line) Sum of black spectrum, 50% of blue spectrum and 50% of red spectrum in panel c. (e) 10 times expanded double difference spectra between Q_B-/Q_B spectra in H_2O and $H_2{}^{18}O$. (black line) Double difference spectra between measured spectra shown in panel b. (red line) Double difference spectra of simulated spectra shown in panel d.

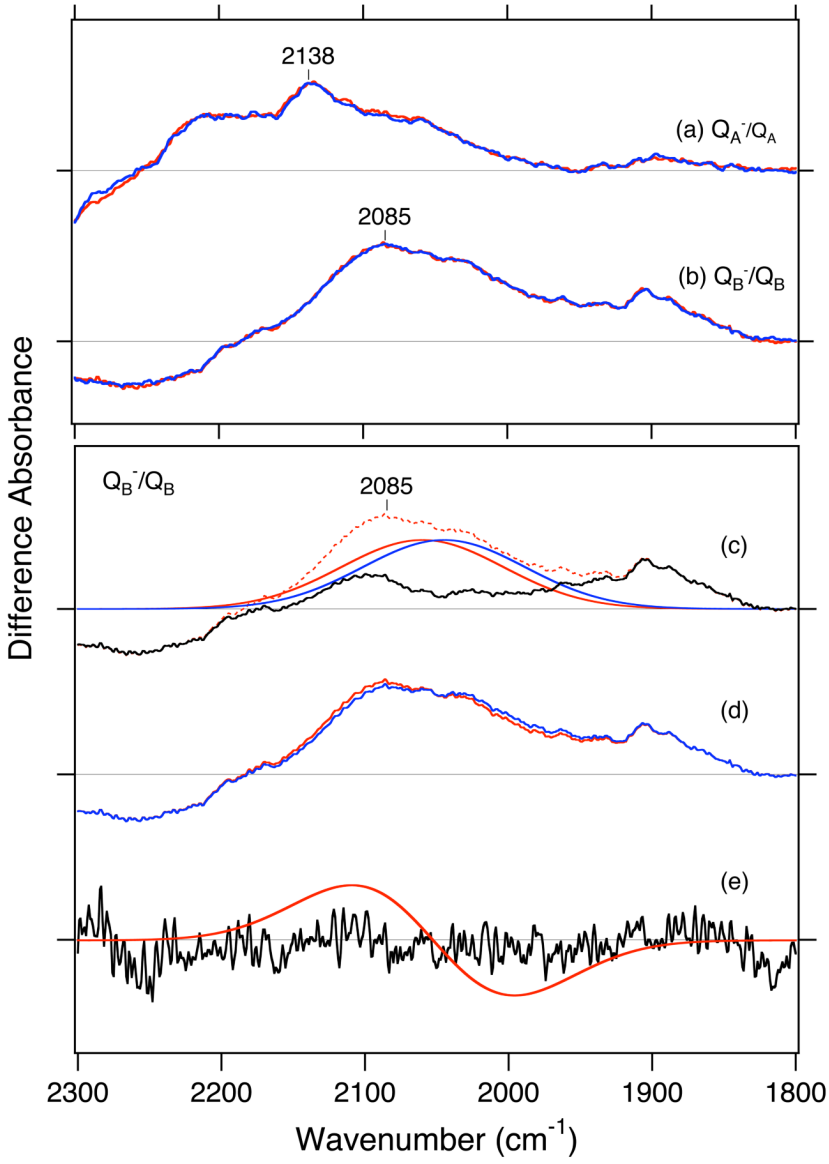

Figure 6.

(a, b)Light-induced Q-/Q difference FTIR spectra of *Rb. Sphaeroides* RCs in the 2300-1800 cm^{-1} region incubated in D_2O buffer. Q_A-/Q_A spectra (a) and Q_B-/Q_B spectra (b) of WT. Samples are hydrated with D_2O (red line) or $D_2{}^{18}O$ (blue line). (c–e) Comparison of observed and simulated Q_B-/Q_B spectra of WT *Rb. sphaeroides* RCs in D_2O and in $D_2{}^{18}O$. (c) (red solid line) The Gaussian function whose position and half maximum full width are 2060 cm^{-1} and 133 cm^{-1}, respectively. (black line) The difference spectrum between red dotted spectrum and red solid spectrum. (blue line) The Gaussian function whose position and half maximum full width are 2045 cm^{-1} and 133 cm^{-1}, respectively. (d) (red line) WT Q_B-/Q_B spectrum (sum of red solid line and black line in panel c). (blue line) Sum of black spectrum, 50% of blue spectrum and 50% of red spectrum in panel c. (e) 10 times expanded double difference spectra between Q_B-/Q_B spectra in D_2O and $D_2{}^{18}O$. (black line) Double difference spectra between measured spectra shown in panel b. (red line) Double difference spectra of simulated spectra shown in panel d.

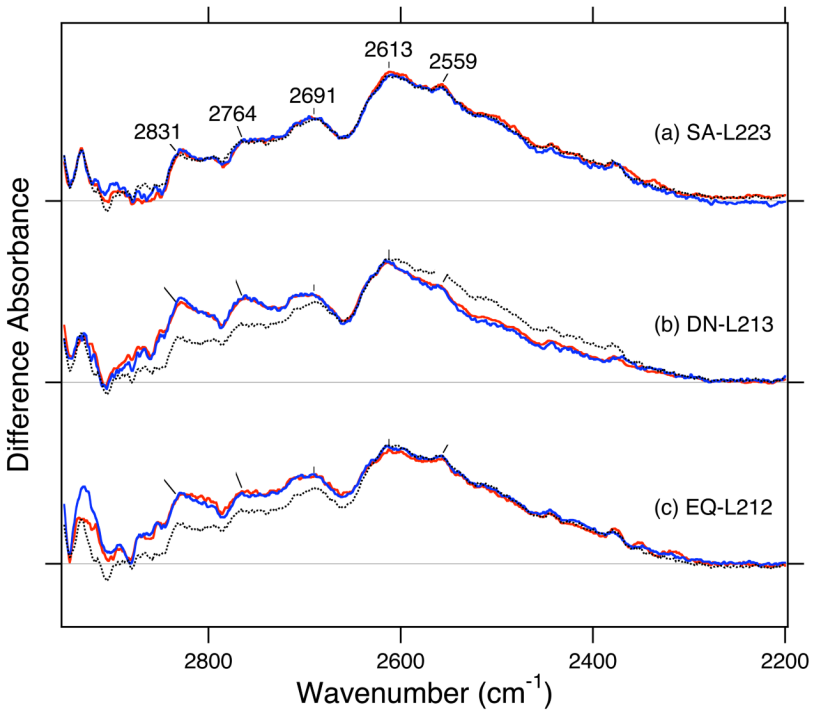

Figure 7.

Light-induced Q_B-/Q_B difference FTIR spectra of *Rb. Sphaeroides* mutant RCs in the 2950-2200 cm^{-1} region. Q_B-/Q_B spectra of SA-L223 (a), DN-L213 (b) and EQ-L212 (c) are shown. Samples are hydrated with H_2O (red line) or $H_2{}^{18}O$ (blue line). Dotted lines in a–c show the Q_B-/Q_B spectra of WT. One division of the *y*-axis corresponds to 0.0003 absorbance unit.

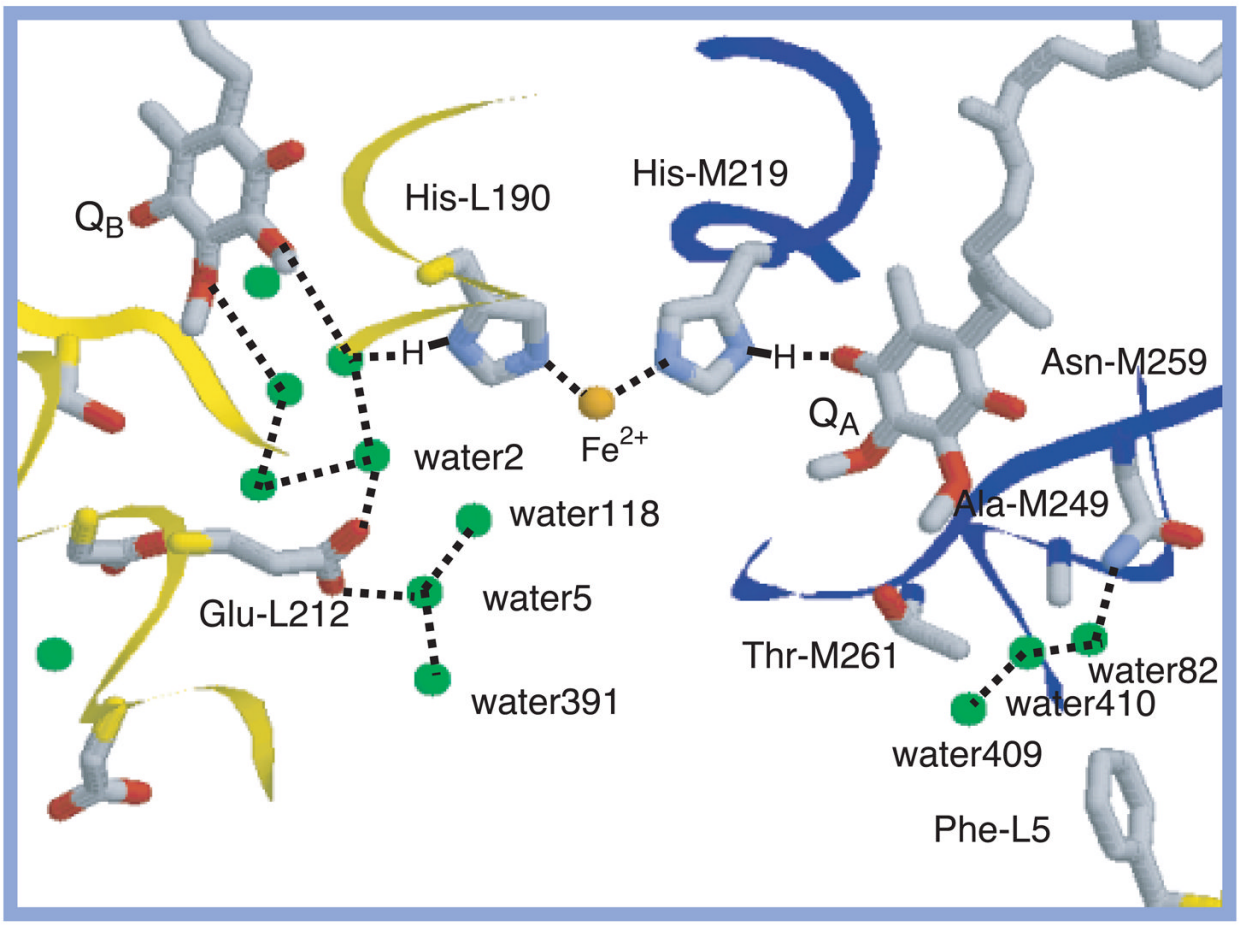

Figure 8.
Structure of quinone binding sites of the reaction center of *Rb. sphaeroides* in the dark state (PDB entry: 1AIJ (10)). Peptide backbones are shown as ribbons, where L and M subunits are colored yellow, blue, respectively. Quinone and amino acid side chains are shown as stick drawings. Green shares represent water molecules. Dotted lines show putative hydrogen bonds.